Available online at www.sciencedirect.com
ScienceDirect
Computational Biology and Chemistry 30 (2006) 327–338
Computational Biology and Chemistry
www.elsevier.com/locate/compbiolchem

Analysis of enzymopathies in the human red blood cells by constraint-based stoichiometric modeling approaches

Saliha Durmuş Tekir, Tunahan Çakır, Kutlu Ö. Ülgen *

Department of Chemical Engineering, Boğaziçi University, 34342 Bebek-İstanbul, Turkey

Received 7 November 2005; received in revised form 10 April 2006; accepted 3 July 2006

Abstract

The human red blood cell (RBC) metabolism is investigated by calculating steady state fluxes using constraint-based stoichiometric modeling approaches. For the normal RBC metabolism, flux balance analysis (FBA) is performed via optimization of various alternative objective functions, and the maximization of production of ATP and NADPH is found to be the primary objective of the RBC metabolism. FBA and two novel approaches, minimization of metabolic adjustment (MOMA) and regulatory on–off minimization (ROOM), which can describe the behavior of the metabolic networks in case of enzymopathies, are applied to observe the relative changes in the flux distribution of the deficient network. The deficiencies in several enzymes in RBC metabolism are investigated and the flux distributions are compared with the non-deficient FBA distribution to elucidate the metabolic changes in response to enzymopathies. It is found that the metabolism is mostly affected by the glucose-6-phosphate dehydrogenase (G6PDH) and phosphoglycerate kinase (PGK) enzymopathies, whereas the effects of the deficiency in DPGM on the metabolism are negligible. These stoichiometric modeling results are found to be in accordance with the experimental findings in the literature related to metabolic behavior of the human red blood cells, showing that human RBC metabolism can be modeled stoichiometrically.

Keywords: Red blood cell; Enzymopathy; Flux balance analysis; Minimization of metabolic adjustment; Regulatory on–off minimization

1. Introduction

The red blood cell (RBC) is, structurally and metabolically, the simplest cell in the body. During its maturation, the RBC loses all its subcellular organelles and depends exclusively on glucose as its fuel. The primary role of RBC glucose metabolism is oxygen transport and delivery. RBC performs several other metabolic functions for its own survival, e.g. the synthesis of some metabolites as cofactors (ATP, NADPH and NADH). Due to its simplicity, accessibility, and detailed knowledge of its molecular components, the energy and the redox metabolism of the human RBC has been investigated extensively and it has an important role in the development of mathematical models of the metabolic networks (Çakır et al., 2004; Holzhütter, 2004; Jamshidi et al., 2001; Joshi and Palsson, 1989; Mulquiney and Kuchel, 1999; Ni and Savageau, 1996; Schuster and Holtzhütter, 1995; Schuster et al., 1998).

In RBC, deficiencies of about 20 enzymes at varying degrees of severity have been identified (Jacobasch and Rapoport, 1996; Jacobasch, 2000; Schuster and Holtzhütter, 1995) that result in serious diseases. Tackling with such diseases is only possible if the biochemical disorders in related enzymes are analyzed well. As it is very difficult to observe experimentally the quantitative effect of the degree of the enzymopathies on the extent of the metabolic disorder, mathematical modeling is generally the preferred tool. The RBC metabolism has been studied by kinetic modeling approaches (Jamshidi et al., 2001; Joshi and Palsson, 1989; Martinov et al., 2000; Mulquiney and Kuchel, 1999; Ni and Savageau, 1996; Schuster et al., 1989; Schuster and Holtzhütter, 1995), which require well-defined kinetic parameters of all enzymes in the metabolic network. Stoichiometric modeling studies have also been performed to analyze the red blood cells (Çakır et al., 2004; Holzhütter, 2004; Price et al., 2003; Schuster et al., 1998; Wiback and Palsson, 2002), which require only the stoichiometries and the reversibility of the reactions in the network.

FBA (Kauffman et al., 2003; Varma and Palsson, 1994) is the preferred stoichiometric modeling approach for underdetermined reaction systems where the number of unknowns (fluxes)

* Corresponding author. Tel.: +90 212 3596869; fax: +90 212 2872460.
E-mail address: ulgenk@boun.edu.tr (K. Ö. Ülgen).

1476-9271/$ – see front matter © 2006 Elsevier Ltd. All rights reserved.
doi:10.1016/j.compbiolchem.2006.07.001

is greater than the number of the independent equations (mass balances around the metabolites). Assuming optimal behavior of the metabolism, FBA uses linear programming with defined constraints and an objective function to calculate the steady state flux distributions. Recently two stoichiometric modeling approaches have been proposed to predict the response of the metabolic networks to changes in enzyme activities; MOMA (Segre et al., 2002) and ROOM (Shlomi et al., 2005), which assume non-optimal behavior for a deficient organism. These approaches identify the behavior of the deficient metabolisms by describing how the flux distributions deviate from the non-deficient ones. MOMA is based on minimizing the metabolic adjustment of the fluxes with respect to the non-deficient case where the Euclidean norm of the flux differences is minimized using quadratic programming (Segre et al., 2002). On the other hand, ROOM minimizes the number of significant flux changes with respect to the non-deficient metabolism with mixed integer linear programming (Shlomi et al., 2005).

The present study focuses on the steady state flux analysis of the human RBC metabolic network using constraint-based stoichiometric modeling methods for both non-deficient and deficient cases. The metabolic function which has the major importance in RBC metabolism was identified by observing the degree of the correlation between the FBA-based flux distribution for different objective functions and the kinetic models (Jamshidi et al., 2001; Mulquiney and Kuchel, 1999; Schuster and Holtzhütter, 1995). The three methods mentioned above (FBA, MOMA and ROOM) were then used to calculate the steady state flux distributions in case of enzyme defects. The results were compared with the non-deficient flux distribution to observe the effect of the deficiencies on the RBC metabolism. This study aims to give light to further research on the identification of possible drug targets to cure the enzymopathies in human red blood cells.

2. Modeling aspects

2.1. Metabolism of the human red blood cell

The human RBC metabolism is depicted in Fig. 1 (Joshi and Palsson, 1989; Schuster et al., 1998) and the reactions used in in silico model are listed in Table 1. There are 36 metabolites in 35 reactions. Seventeen of the reactions are reversible and there are six extracellular metabolites; glucose and adenine are taken as the inputs to the system and lactate, HYPX, D23PG and CO_2 are taken as the outputs from the system. In G6PDH and TPI enzymopathies, R5P and DHAP were also taken as the outputs, respectively, as these metabolites were reported to be secreted from RBC in case of corresponding deficiencies (Çakır et al., 2004).

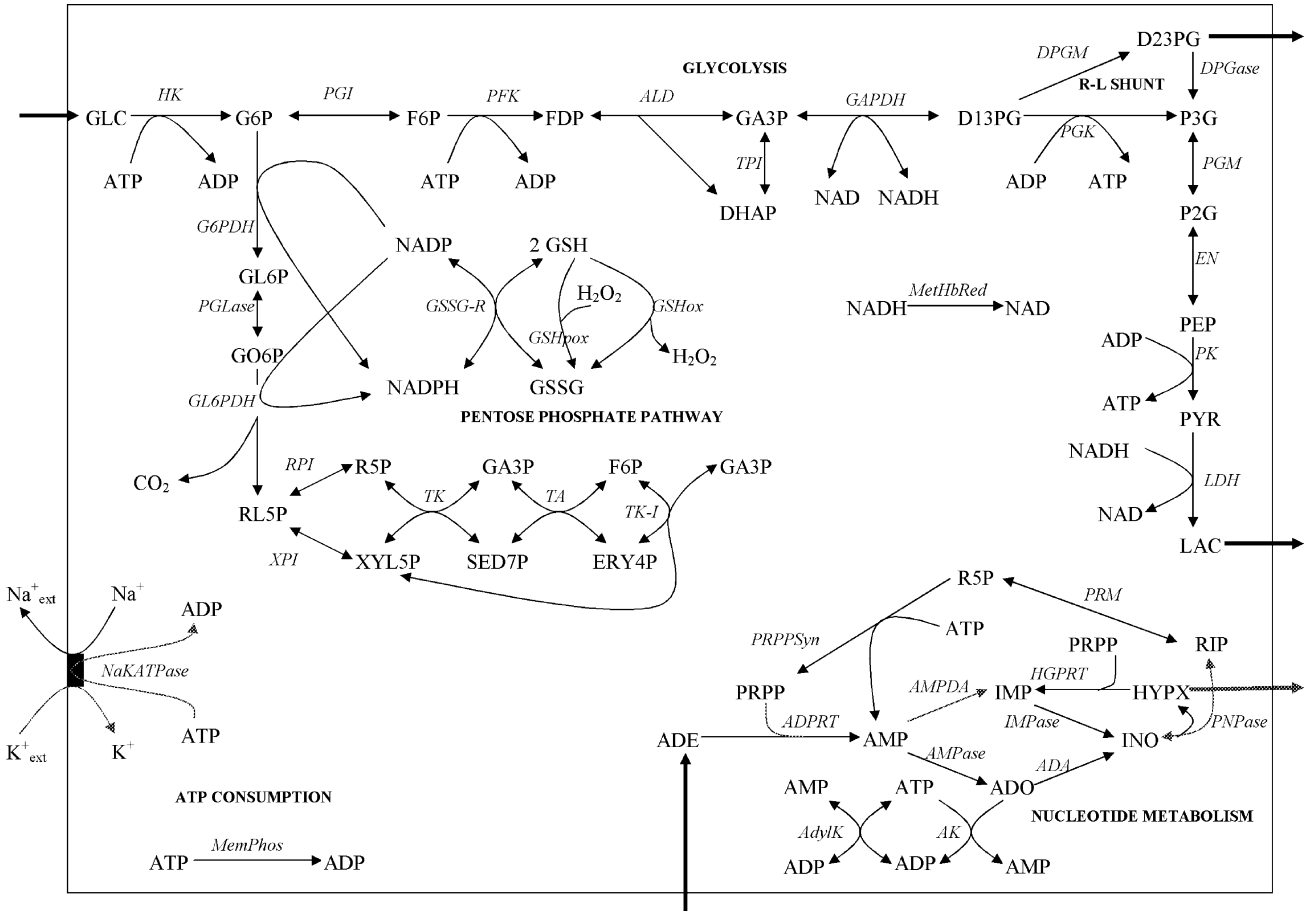

Fig. 1. The human RBC metabolism (adapted from Schuster et al., 1998).

Table 1
Reactions in RBC metabolism with corresponding enzymes

Reactions		Enzymes
Glycolysis		
1GLC + 1ATP → 1G6P + 1ADP	(1)	HK
1G6P ↔ 1F6P	(2)	PGI
1F6P + 1ATP → 1FDP + 1ADP	(3)	PFK
1FDP ↔ 1GA3P + 1DHAP	(4)	ALD
1DHAP ↔ 1GA3P	(5)	TPI
1GA3P + 1NAD ↔ 1D13PG + 1NADH	(6)	GAPDH
1D13PG + ADP ↔ 1P3G + 1ATP	(7)	PGK
1P3G ↔ 1P2G	(8)	PGM
1P2G ↔ 1PEP	(9)	EN
1PEP + 1ADP → 1PYR + 1ATP	(10)	PK
1PYR + 1NADH → 1LAC + 1NAD	(11)	LDH
Rapoport–Luebering shunt		
1D13PG → 1D23PG	(12)	DPGM
1D23PG → 1P3G	(13)	DPGase (DPGM)
Pentose phosphate pathway		
1G6P + 1NADP → 1GL6P + 1NADPH	(14)	G6PDH
1GL6P ↔ 1GO6P	(15)	PGLase
1GO6P + 1NADP → 1RL5P + 1NADPH + 1CO_2	(16)	GL6PDH
1RL5P ↔ 1XYL5P	(17)	XPI
1RL5P ↔ 1R5P	(18)	RPI
1R5P + 1XYL5P ↔ 1SED7P + 1GA3P	(19)	TK
1SED7P + 1GA3P ↔ 1F6P + 1ERY4P	(20)	TA
1XYL5P + 1ERY4P ↔ 1F6P + 1GA3P	(21)	TK-I
Nucleotide metabolism		
1R5P + 1ATP → 1PRPP + 1AMP	(22)	PRPPsyn
1R1P ↔ 1R5P	(23)	PRM
1PRPP + 1ADE → 1AMP	(24)	ADPRT
1INO ↔ 1HYPX + R1P	(25)	PHPase
1HYPX + 1PRPP → 1IMP	(26)	HGPRT
1IMP → 1INO	(27)	IMPase
1AMP → 1ADO	(28)	AMPase
1AMP → 1IMP	(29)	AMPDA
1ADO → 1INO	(30)	ADA
1ADO + 1ATP → 1ADP + 1AMP	(31)	AK
2ADP ↔ 1ATP + 1AMP	(32)	AdylK
Cellular functions		
1GSSG + 1NADPH ↔ 2GSH + 1NADP	(33)	GSSG-R
ATP → ADP	(34)	MemPhos
MetHb + NADH → Hb + NAD	(35)	MetHbRed

The red blood cell metabolizes glucose through glycolysis pathway anaerobically yielding 2 mol of ATP and lactate/mol of glucose. In red blood cells the anaerobic glycolysis is modified by the Rapoport–Luebering (R–L) shunt producing 2,3-diphosphoglycerate (D23PG) (Bossi and Giardina, 1996; Momsen and Vestergaard-Bogind, 1978). The pentose phosphate pathway (PPP) controls the redox status of the cell yielding 2 mol NADPH/mol of glucose. The red blood cell requires ATP for nucleotide metabolism and cellular functions.

2.2. Constraint-based stoichiometric modeling approaches

2.2.1. FBA

Flux balance analysis (FBA) (Kauffman et al., 2003; Varma and Palsson, 1994) is an optimization method to calculate steady state flux distribution (v) maximizing an objective function (f) using linear programming (LP) with the formulation:

$$\max\ f^{\mathrm{T}} \cdot v$$
$$\text{s.t. } \boldsymbol{S} \cdot v = \boldsymbol{b}, \quad v_{\min} \le v \le v_{\max}$$

The red blood cell metabolism described in Section 2.1 was defined by the stoichiometric matrix, $\boldsymbol{S}$, that shows the effect of all fluxes on metabolites representing the mass balance constraints. The reversible reactions were split into forward and backward reactions, to deal with non-negative flux values ($v_{\min}$ is zero and $v_{\max}$ is infinity). The resulting net fluxes of the reversible reactions may have both signs. The dimension of constructed $\boldsymbol{S}$ matrix is 36×58 where 36 is the number of the metabolites and 58 is the total number of fluxes including 35 forward, 17 backward and 6 exchange fluxes. The matrix has an additional column for secretion fluxes of R5P or DHAP from the cell in case of G6PDH and TPI enzymopathies, respectively; otherwise these metabolites were taken as intracellular. For the intracellular metabolites, pseudo steady state was assumed and the accumulation of only extracellular metabolites was considered. In the accumulation vector ($\boldsymbol{b}$), only the entries corresponding to the extracellular metabolites are nonzero. As the objective functions, the minimization of the total fluxes in the network (Bonarius et al., 1996; Holzhütter, 2004) and individual or combined maximization of production of several desired metabolites (ATP, NADH, NADPH and D23PG) was used in FBA calculations for the RBC metabolism (see Section 3.1).

2.2.2. MOMA

Assuming optimal behavior of a deficient organism may not adequately represent the real behavior (Segre et al., 2002; Shlomi et al., 2005). Segre et al. (2002) proposed the method of minimization of metabolic adjustment (MOMA) where deficient metabolic fluxes are adjusted by a minimal redistribution with respect to the non-deficient flux distributions. MOMA uses quadratic programming (QP) to search the point (v) in the flux space, which has the smallest Euclidean distance to the non-deficient flux solution that is found from FBA (w). MOMA can be formalized as:

$$\min\,(v-w)^{\mathrm{T}} \cdot (v-w)$$
$$\text{s.t. } \boldsymbol{S} \cdot v = \boldsymbol{b}, \quad v_{\min} \le v \le v_{\max}$$

The value of v_j, where jth flux is associated with a totally or partially deficient enzyme, is specified as a percentage of its non-deficient value found from FBA calculations. In MOMA the system is subjected to the same stoichiometric constraints as in FBA, but MOMA does not assume optimal behavior. A deficient cell is likely to have a suboptimal flux distribution that is intermediate between healthy optimum and the diseased optimum, and MOMA provides an approximation for this suboptimal state (Segre et al., 2002).

2.2.3. ROOM

As the Euclidean norm of the flux differences between the non-deficient and the deficient organism is minimized in MOMA approach, large modifications in single fluxes in deficiency cases are prevented (Shlomi et al., 2005). However, such large flux changes may be required to reroute the metabolic fluxes through

alternative pathways, as observed experimentally (Emmerling et al., 2002). Recently Shlomi et al. (2005) proposed that minimizing the number of significant flux changes (on/off) with respect to the non-deficient flux distribution reflects the true behavior of the deficient metabolic networks introducing the method, regulatory on–off minimization (ROOM). As opposed to MOMA, ROOM permits large modifications in single fluxes. To find the ROOM solution in a deficiency case, the non-deficient flux distribution (w) is first found with FBA and a small range $[w^l, w^u]$ is defined around these fluxes allowing the non-significant flux changes. The optimization performs the minimization of the number of the deficient flux value, which is out of the defined range. ROOM approach uses mixed integer linear programming (MILP) based on the formulation:

$$\min \sum_{i=1}^{m} y_i, \quad y_i \in \{0, 1\}$$

$$\text{s.t. } \boldsymbol{S} \cdot v = \boldsymbol{b}$$

$$v - y \cdot (v_{\max} - w^u) \leq w^u \tag{1}$$

$$v - y \cdot (v_{\min} - w^l) \geq w^l \tag{2}$$

$$w^u = w + \delta \cdot |w| + \in, \quad w^l = w - \delta \cdot |w| + \in$$

where for each flux i, $1 \leq i \leq m$, $y_i = 1$ for a significant flux change in v_i, and $y_i = 0$ otherwise. When $y_i = 1$, the flux values in deficiency cases are subjected to only the constraint $v_{\min} \leq v \leq v_{\max}$. If $y_i = 0$, (1) and (2) constrain v_i to the range around the non-deficient flux value defined above. δ and $\in$ represents the relative and absolute ranges of tolerance, respectively (Shlomi et al., 2005), and we used $\delta = 0.05$ and $\in = 0.0001$ in ROOM calculations.

In this study, all optimization problems were solved via TOMLAB's CPLEX solver in MATLAB 7.0.

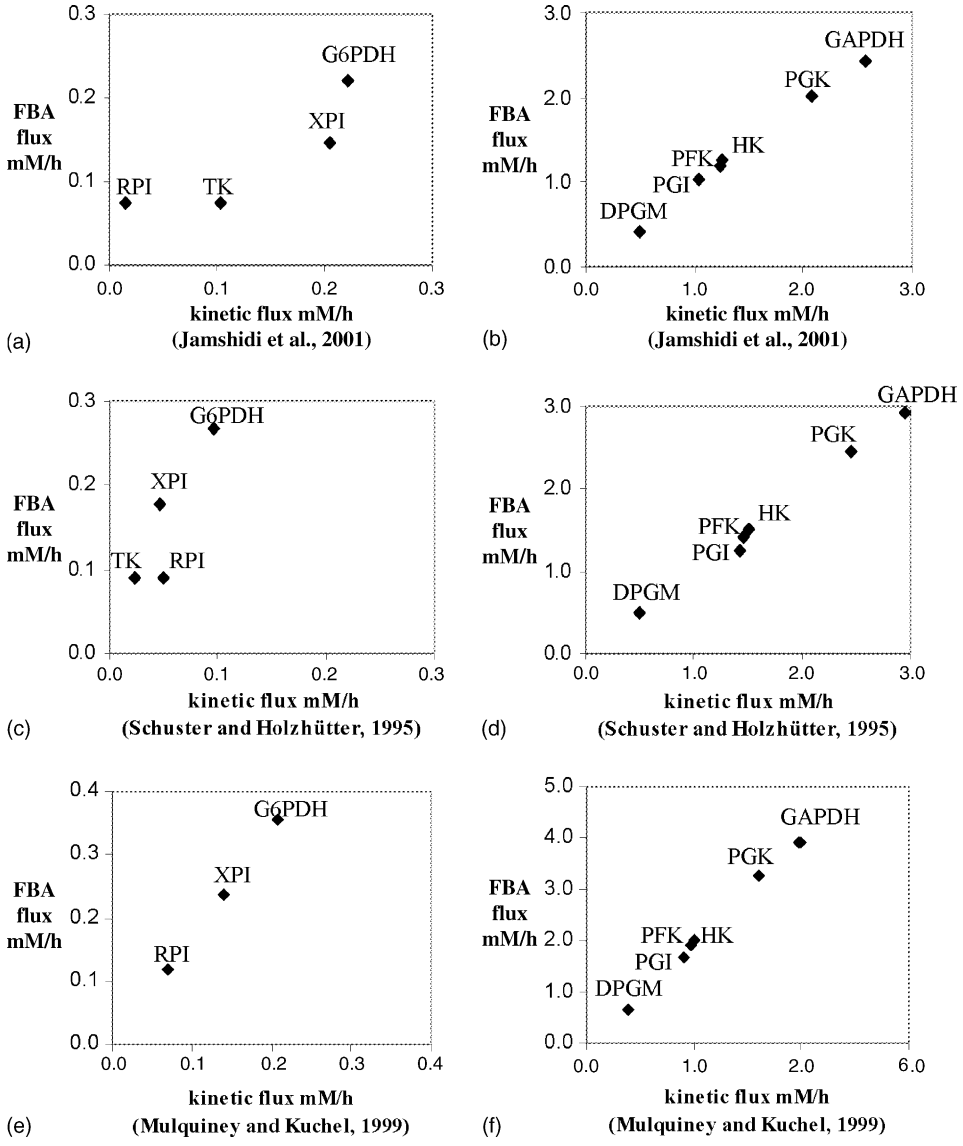

Fig. 2. Comparison of non-deficient flux distributions obtained by FBA with objective function of ATP + NADPH maximization and by the kinetic models.

3. Results

3.1. Identification of objective function

To define the metabolic function having major importance in the RBC metabolism, the steady state flux distributions were calculated by FBA using various physically meaningful objective functions, i.e. minimization of the total fluxes (Bonarius et al., 1996; Holzhütter, 2004), maximization of ATP, maximization of NADPH and maximization of ATP and NADPH, maximization of all ATP, NADH, NADPH and D23PG since the production of these metabolites are crucial for the functioning of RBC metabolism. Only the stoichiometries and the reversibility of the reactions were used in the optimization calculations without any kinetic parameter requirement.

The flux values for the inputs (glucose and adenine) were obtained from the kinetic models (Jamshidi et al., 2001; Mulquiney and Kuchel, 1999; Schuster and Holtzhütter, 1995) and specified in the FBA calculations. The flux of the first reaction of R–L shunt, phosphorylation of D23PG (r_{12}) was restricted to be in 33–40% of the glucose uptake rate. The flux of the first reaction of PPP, oxidation of G6P and reduction of NADH producing NADPH (r_{14}), was constrained to be in the range of 7–18% of glucose flux. These values are the highest and the lowest percentage of glucose uptake rate for fluxes of r_{12} and r_{14} in the kinetic models (Jamshidi et al., 2001; Mulquiney and Kuchel, 1999; Schuster and Holtzhütter, 1995).

In order to assess the optimization results with different objective functions, the steady state flux values of the human red blood cells computed by FBA for each objective function were compared with those of the kinetic models. The sta-

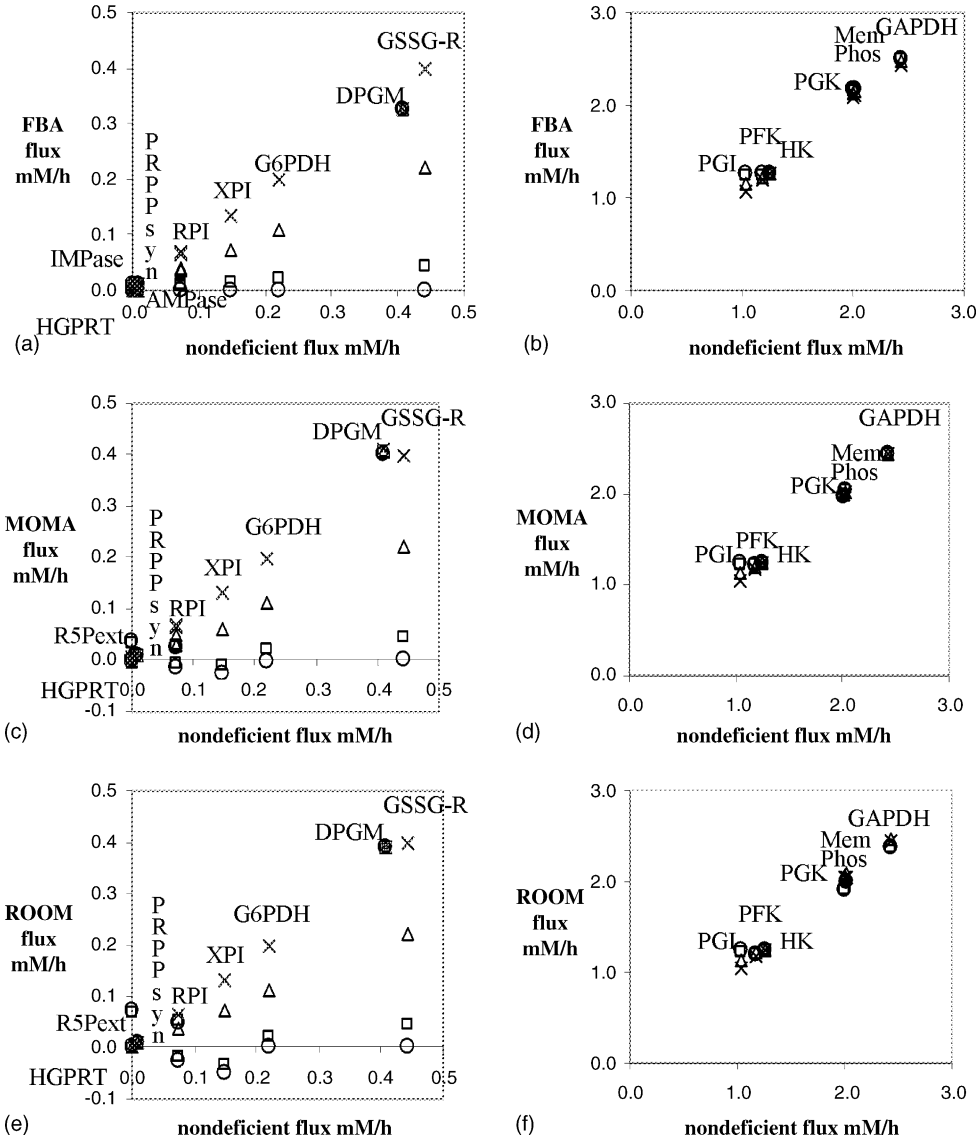

Fig. 3. Comparison of flux distributions with G6PDH deficiency at varying degrees obtained by FBA, MOMA, ROOM and non-deficient flux distribution obtained by FBA. (◯) G6PDH flux is 0% of its non-deficient value; (□) G6PDH flux is 10% of its non-deficient value; (△) G6PDH flux is 50% of its non-deficient value; (×) G6PDH flux is 90% of its non-deficient value. Slopes of the correlation lines ($y = m \times x$) between deficient flux distributions and non-deficient flux distribution and the corresponding correlation coefficients (R^2) can be found in Supplementary Table 1a.

tionary flux distributions of the glycolysis pathway including Rapoport–Luebering shunt and the pentose phosphate pathway were used in these comparisons since the models of Mulquiney and Kuchel (1999) and Schuster and Holtzhütter (1995) do not include the nucleotide metabolism. FBA results with maximization of ATP and NADPH production gave the best correlation with the kinetic models. The high (glycolysis and R–L shunt) and low flux values (PPP) were plotted separately for better visualization (Fig. 2). ATP and NADPH are necessary cofactors for the RBC metabolism. ATP is required to maintain osmotic balance of the cell (Bossi and Giardina, 1996; Schilling and Palsson, 1998) and NADPH is obligatory to protect the cell against oxidative damage (Jacobasch and Rapoport, 1996).

3.2. Analysis of enzymopathies

G6PDH, TPI, PGI, PGK and DPGM were taken as the model enzymopathies. For the analysis of deficiencies of these enzymes, the constructed stoichiometric model was solved using the constraint-based methods of FBA, MOMA and ROOM. The steady state flux distributions in case of enzymopathies were compared with those of the non-deficient distributions given in Fig. 2a and b. The reaction set of the kinetic model developed by Jamshidi et al. (2001) includes nucleotide metabolism and thus it was considered to be the most similar to our set of the stoichiometric model reactions.

In the deficiency analyses, none of the reactions was restricted to be in any boundaries other than reversibility constraints. In FBA calculations only, the differences between the non-deficient and deficient fluxes of r_{12} and r_{14} were minimized to force the cell to be within the boundaries as it was in the healthy case. The violation of the non-deficient boundaries was used as a measure to judge the severeness of the deficiencies.

FBA, the oldest and most widely utilized method, assumes optimal behavior of metabolism even in deficient cases, whereas MOMA and ROOM assume non-optimal behavior. However, the

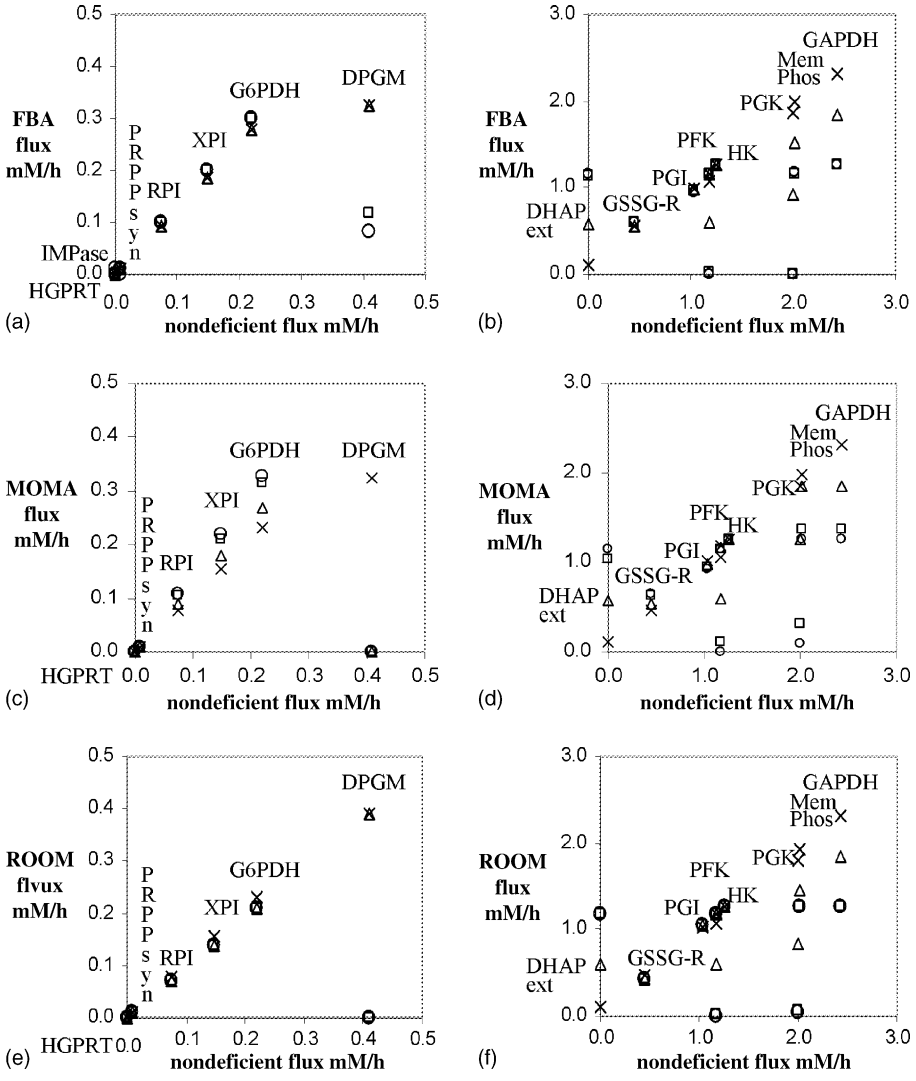

Fig. 4. Comparison of flux distributions with TPI deficiency at varying degrees obtained by FBA, MOMA, ROOM and non-deficient flux distribution obtained by FBA. (◯) TPI flux is 0% of its non-deficient value; (□) TPI flux is 10% of its non-deficient value; (△) TPI flux is 50% of its non-deficient value; (×) TPI flux is 90% of its non-deficient value. Slopes of the correlation lines ($y = m \times x$) between deficient flux distributions and non-deficient flux distribution and the corresponding correlation coefficients (R^2) can be found in Supplementary Table 1b.

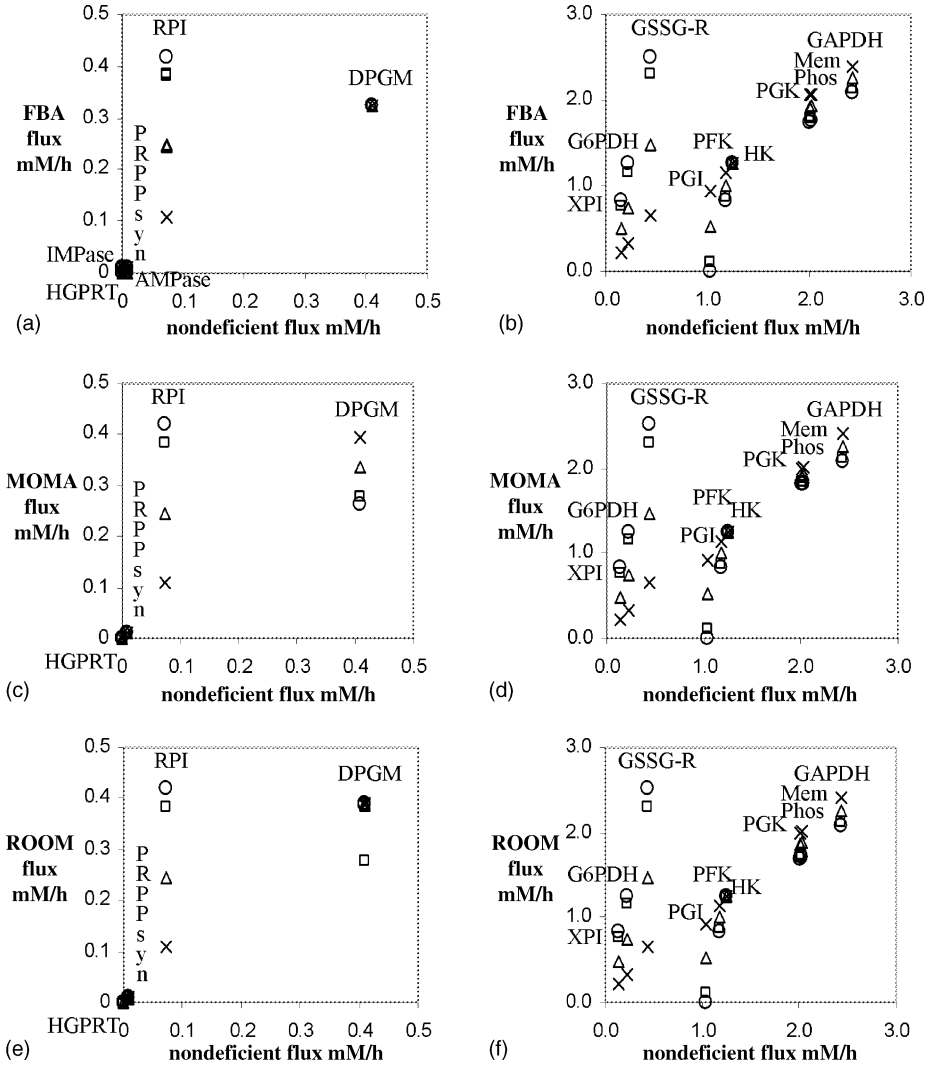

Fig. 5. Comparison of flux distributions with PGI deficiency at varying degrees obtained by FBA, MOMA, ROOM and non-deficient flux distribution obtained by FBA. (◯) PGI flux is 0% of its non-deficient value; (□) PGI flux is 10% of its non-deficient value; (△) PGI flux is 50% of its non-deficient value; (×) PGI flux is 90% of its non-deficient value. Slopes of the correlation lines ($y = m \times x$) between deficient flux distributions and non-deficient flux distribution and the corresponding correlation coefficients (R^2) can be found in Supplementary Table 1c.

flux distributions obtained by these constraint-based methods are similar to each other except a few cases (Figs. 3–7). This is probably because of the simplicity of the red blood cell metabolism, reflected in the number of involved reactions (Table 1) compared to the recent genome-scale models with more than 700 reactions (Förster et al., 2003; Sheikh et al., 2005). Moreover, FBA does not take any regulatory constraint into account, whereas MOMA and ROOM include regulatory constraints implicitly. The similarity in the results indicates that the RBC metabolism works properly without regulatory constraints since RBC responds to perturbations in a similar manner with (FBA) or without (MOMA and ROOM) regulatory constraints.

3.2.1. G6PDH

It can be observed that one of the most severe enzymopathies is the deficiency of glucose-6-phosphate dehydrogenase (G6PDH) (Figs. 3 and 8). This enzyme catalyzes the first reaction of the pentose phosphate pathway (r_{14}) producing NADPH, which has an important role in glutathione system to protect the cell against oxidative stress. The main function of the PPP is to synthesize ribose, components of nucleotides, and NADPH (Jacobasch and Rapoport, 1996). At 90% of the non-deficient G6PDH flux, the metabolism is not affected dramatically. However, with increasing levels of deficiencies, all fluxes of PPP decline with the critical glutathione reductase reaction resulting in low NADPH production. At the high deficiency states, the cell does not function properly and dies.

3.2.2. TPI

Triose phosphate isomerase (TPI) catalyzes the reversible conversion of dihydroxy-acetone (DHAP) to glyceraldehyde-3-phosphate (GA3P) (r_5). This enzymopathy has been reported as crucial because of the high levels of DHAP, which is toxic for cellular functions (Jacobasch and Rapoport, 1996; Orosz et al., 1996; Schneider, 2000). TPI defects in RBC metabolism cause hemolytic anemia with neurological dysfunction (Olah et al.,

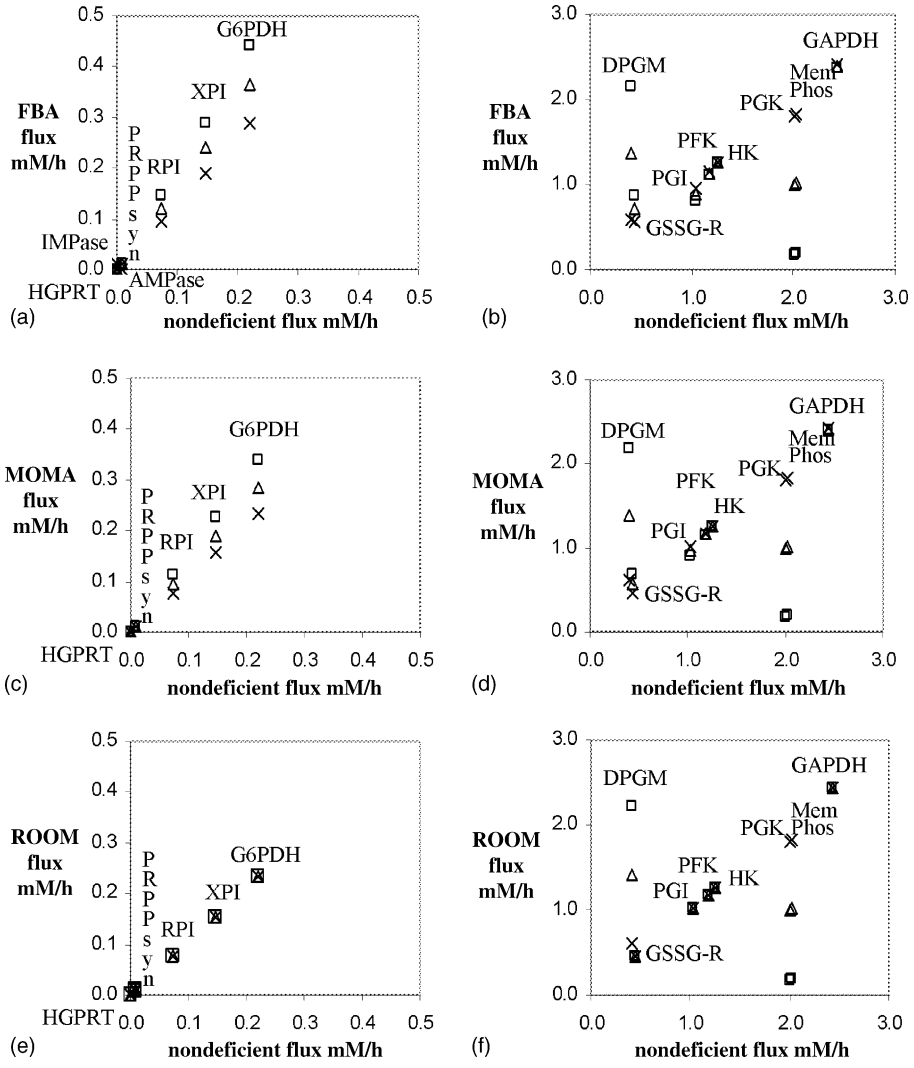

Fig. 6. Comparison of flux distributions with PGK deficiency at varying degrees obtained by FBA, MOMA, ROOM and non-deficient flux distribution obtained by FBA. (□) PGK flux is 10% of its non-deficient value; (△) PGK flux is 50% of its non-deficient value; (×) PGK flux is 90% of its non-deficient value. Slopes of the correlation lines ($y = m \times x$) between deficient flux distributions and non-deficient flux distribution and the corresponding correlation coefficients (R^2) can be found in Supplementary Table 1d.

2002). With increasing levels of TPI deficiency, high DHAP flux was observed and the glycolysis fluxes were found to decrease, whereas PPP fluxes were found to increase (Fig. 4). The glycolytic pathway was found to be completed even in the lack of TPI, to yield lactate since GA3P is produced in the PPP (r_{19}, r_{20}). At total deficiency of TPI, the fluxes through these GA3P producing reactions increase to nearly 1.5-fold with respect to the normal fluxes. Another evidence to conclude the severity of TPI enzymopathy for RBC is the violation of non-deficient boundaries of DPGM and G6PDH reactions. Taking DHAP as external led to flux distributions with complete glycolysis in parallel with clinical findings (Repiso et al., 2002) as opposed to the incomplete glycolytic pathway when it is not allowed to be secreted.

3.2.3. PGI

Phosphoglucose isomerase (PGI) deficiency is the third commonly encountered enzymopathy throughout the world (Kannoo et al., 1998). PGI catalyzes the isomerization of G6P to F6P (r_2). PGI defects in RBC were reported to cause decreases in glycolytic fluxes with low lactate formation (Jacobasch and Rapoport, 1996) and increased PPP activities (Kannoo et al., 1998). In the present simulation, the rates of glycolysis reactions decrease resulting in low lactate yield, whereas the rates of PPP reactions increase in accordance with the above observations (Fig. 5). Even though it is one of the enzymes at the initial steps of the glycolysis, the pathway was found to be completed even in total deficiency. In Çakır et al. (2004), elementary flux modes (EFM) analysis resulted in modes with complete glycolytic pathway, which is in parallel with the results of the stoichiometric modeling methods in this study. This is because F6P, the product of r_2, can also be produced by two reactions in the PPP (r_{20}, r_{21}). Therefore, a considerable increase is observed in the rates of these reactions (nearly six-fold in total deficiency). On the other hand, it does not cause any change in the nucleotide metabolism. The PGI enzymopathy leads to a flux distribution in which DPGM and G6PDH fluxes are outside of the non-deficient boundaries.

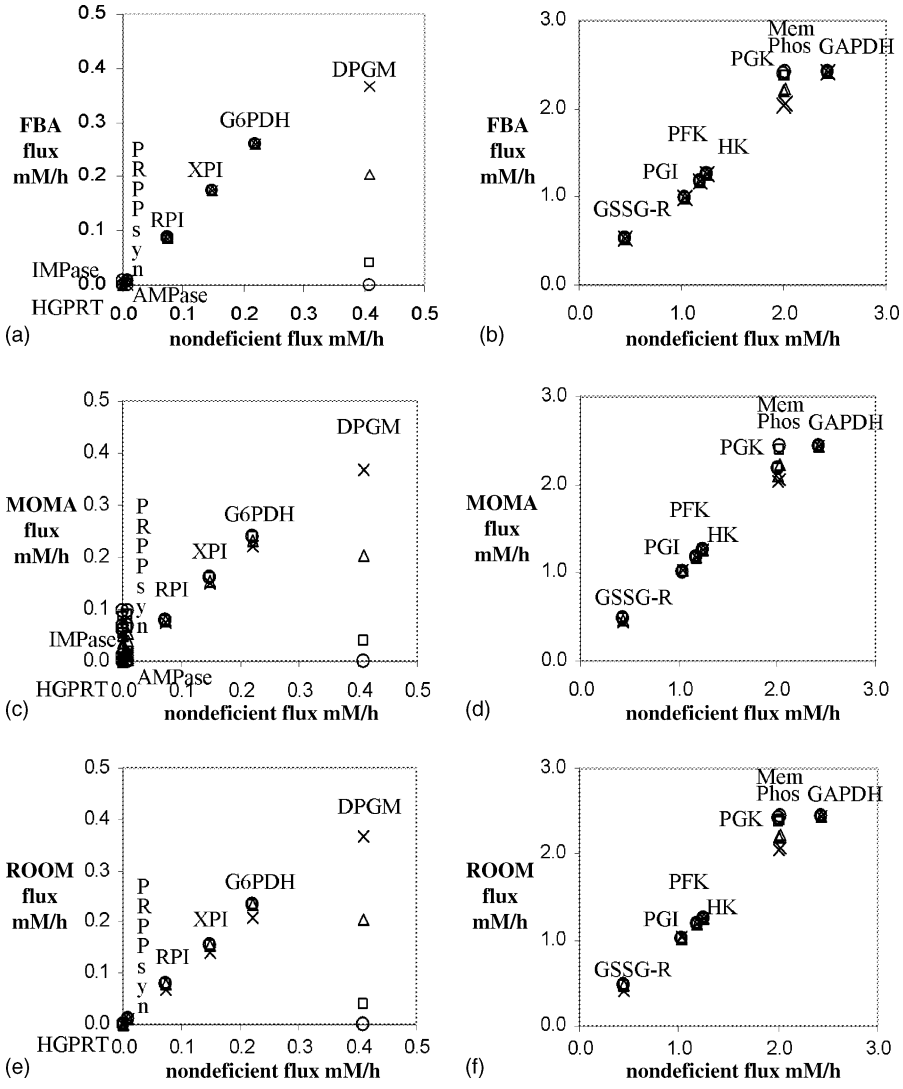

Fig. 7. Comparison of flux distributions with DPGM deficiency at varying degrees obtained by FBA, MOMA, ROOM and non-deficient flux distribution obtained by FBA. (◯) DPGM flux is 0% of its non-deficient value; (□) DPGM flux is 10% of its non-deficient value; (△) DPGM flux is 50% of its non-deficient value; (×) DPGM flux is 90% of its non-deficient value. Slopes of the correlation lines ($y = m \times x$) between deficient flux distributions and non-deficient flux distribution and the corresponding correlation coefficients (R^2) can be found in Supplementary Table 1e.

3.2.4. PGK

Phosphoglycerate kinase (PGK) is crucial for red blood cells since it is one of the enzymes producing ATP, which is required for the cell life. PGK catalyzes the conversion of D13PG (1,3-diphosphoglycerate) to P3G (3-phosphoglycerate) (r_7) bypassing Rapoport–Luebering shunt. Decreased concentration of ATP (Fujii and Miwa, 2000) and low glucose consumption (Jacobasch, 2000) are observed in patients with PGK deficiency. Similar to the results of TPI and PGI deficiencies, PGK deficiency causes a decrease in glycolytic fluxes resulting in a decline of ATP flux and an increase in PPP fluxes (Figs. 6 and 9). However, when the PGK flux is fully blocked the glycolytic pathway was found to be incomplete. When PGK flux is constrained to be zero the constraint-based modeling methods are unable to simulate the case and the model does not have a solution with an incomplete glycolytic pathway. PGK enzymopathy also forces the blood cell to violate the non-deficient boundaries of DPGM and G6PDH fluxes. In this case, different from the TPI and PGI deficiencies, the deviation of the flux through the DPGM reaction is large with respect to the non-deficient value.

3.2.5. DPGM

The minute effects on RBC metabolism that DPGM deficiency causes can be observed in Fig. 7. It affects only the Rapoport–Luebering shunt as no considerable changes occur in other parts of the network even when no DPGM exists. The results show that it is the least crucial enzymopathy, which is in accordance with the clinical findings (Jacobasch and Rapoport, 1996).

3.3. Effects of enzymopathies on RBC metabolism

To determine the degree of the effect of enzymopathies on the metabolism, one should know how they affect the objective function. The primary objective of the RBC was determined as the

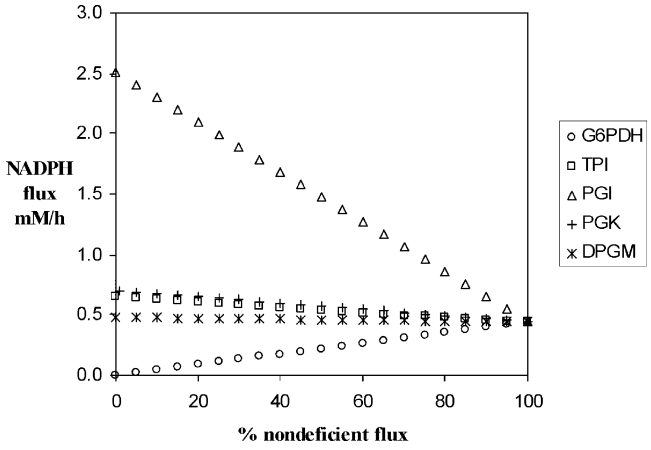

Fig. 8. Effects of the enzymopathies on NADPH flux.

maximization of the production of ATP and NADPH. Therefore, the changes in the flux of these molecules due to the deficiencies are crucial for the continuity of the blood cells (Figs. 8 and 9). In G6PDH enzymopathy a continuous decrease in NADPH production is observed with increasing levels of deficiency. Except very low levels of deficiency the cell cannot survive with this enzymopathy because of the lack of NADPH. Defects in TPI result in high NADPH and low ATP fluxes. Since ATP is required for cellular functions this enzymopathy can disturb the cell drastically. The trend is same for the PGI defective metabolism, i.e. increase in NADPH and decrease in ATP production. NADPH flux is more than five-fold of the non-deficient value, and ATP flux decreases to 85% of the non-deficient case. The effect of PGK defects is again increased in NADPH and decreased in ATP. In this case the situation is worse for the cell because of the role of PGK in ATP production in glycolytic pathway. PGK defects directly inhibit the production of ATP. Therefore, PGK is another crucial enzyme for the human red blood cell metabolism. Minute changes are observed in DPGM deficiencies. Even at 100% deficiency, the amounts of ATP and NADPH are nearly equal to the non-deficient values.

The results show that the effect of a deficiency can usually be coped with an enhanced NADPH production, as seen for TPI, PGI and PGK deficiencies. The only case that the cell cannot resist deficiency is when it is directly related to NADPH production (G6PDH enzymopathy). Otherwise, the cell can fight with the deficiencies by activating its osmotic stress protection mechanism (i.e. NADPH production). The other objective of the cell, i.e. ATP production is usually associated with a decrease hinting at the low capacity of the human red blood cells in fighting with changes in energy related mechanisms.

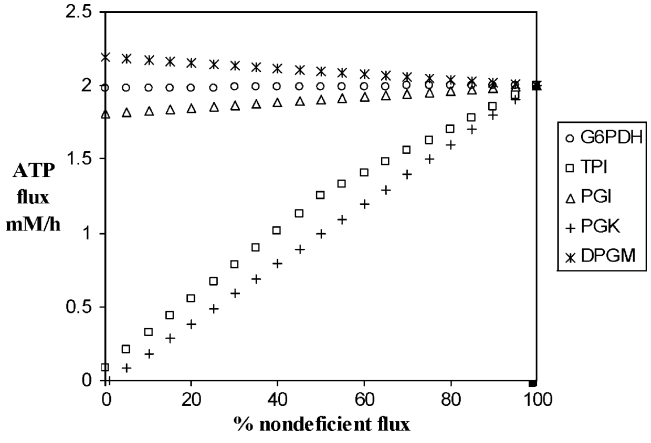

Fig. 9. Effects of the enzymopathies on ATP flux.

The results of this study are in parallel with the clinical facts reported for G6PDH, TPI, PGI, PGK and DPGM enzymopathies showing the prediction power of the constraint-based stoichiometric modeling methods. In the present work, in addition to the five enzymopathies mentioned above, the deficiencies in glyceraldehyde-3-phosphatedehydrogenase (GAPDH), phosphoglycerate mutase (PGM), transketolase (TK) and adenosine deaminase (ADA) were also analyzed with the constraint-based models (figures not shown). The effects of the deficiencies in GAPDH and PGM are similar to other glycolysis enzymes, i.e. a decrease in ATP production and an increase in NADPH production. The observed large deviation of the deficient fluxes from the non-deficient distribution indicates that GAPDH and PGM enzymopathies are crucial for the continuity of the RBC life. Since the inhibition of ATP production is more serious in PGM deficient cells, one can say that the PGM enzymopathy is more defective than GAPDH enzymopathy. Compared to the enzymes analyzed before, the PGM enzymopathy can be considered as crucial as PGK enzymopathy. Deficiencies in TK, which is an enzyme in PPP, resulted in inhibition of the PPP fluxes as expected. Because of the decreased NADPH production, the cell cannot survive at high levels of TK enzymopathy as it was the case for G6PDH deficiency. The defects in ADA affect only the nucleotide metabolism. In ADA enzymopathy, the fluxes of glycolysis and PPP do not deviate from the non-deficient values.

4. Conclusions

The human RBC metabolism was investigated using constraint-based stoichiometric modeling approaches. The metabolic function having major importance in RBC metabolism was identified as the maximization of the production of ATP and NADPH since the results of FBA of the non-deficient metabolism with this objective function gave the best correlation with the kinetic models. The enzymopathies of G6PDH, TPI, PGI, PGK and DPGM were analyzed by three methods; FBA, MOMA and ROOM which gave similar results for high flux carrying reactions, whereas clear differences were observed in the low flux carrying pathways. The detected overall similarity among the different stoichiometric constraint-based methods points to the fact that RBC metabolism generally functions in an optimized way in deficient conditions.

The effect of enzymopathies on the identified objectives (ATP and NADPH; Figs. 8 and 9) of the cell was found to be generally in qualitative agreement with the findings reported in our earlier study (Çakır et al., 2004), which utilizes all possible flux distributions (elementary flux modes, EFMs) with weighted efficiencies to judge the overall effect of these enzymopathies on the metabolism. That study utilizes ATP, NADPH, NADH and D23PG production as the objective function to weight the EFMs.

The present work shows that use of a single flux distribution which obeys the identified objective function has also the capability to model the cell behavior, with special emphasis on the comparison of recently proposed FBA variants for the deficiencies and mutations.

In the present study, G6PDH and PGK were found to be crucial enzymes for the continuity of the RBC since production of essential metabolites (NADPH and ATP) is inhibited with these enzymopathies. The deficiencies in the glycolytic enzymes, TPI and PGI, cause a decrease in glycolysis rates with an increase in PPP rates resulting inhibition of ATP and enhancement of NADPH production. The comparison of the deficient ATP fluxes with the non-deficient ones leads to the conclusion that TPI deficiency is more severe than PGI. DPGM was observed to be the least critical enzyme for the RBC metabolism since its deficiency does not cause dramatic changes in the flux distributions. This work shows the affected fluxes in RBC metabolism in different enzymopathy cases, which can be used as targets for further research to develop drugs for these enzymopathies.

Acknowledgements

We are grateful to Eytan Ruppin for his comments on the results of the deficiency analyses. The financial support for this research was provided by the Boğazici University Research Fund through project no. 05HA502. The doctoral scholarship for Tunahan Çakır, provided within the framework of the integrated Ph.D. program sponsored by BAYG-TUBITAK, is gratefully acknowledged.

Appendix A

Abbreviations for metabolites

ADE adenine
ADO adenosine
D13PG 1,3-biphosphoglycerate
D23PG 2,3-diphosphoglycerate
DHAP dihydroxyacetone phosphate
ERY4P erythrose 4-phosphate
F6P fructose-6-phosphate
FDP fructose diphosphate
G6P glucose-6-phosphate
GA3P glyceraldehydes-3-phosphate
GL6P 6-phosphogluco lactone
GLC glucose
GO6P 6-phosphogluconate
GSH reduced glutathione
GSSG oxidized glutathione
H_2O_2 hydrogen peroxide
Hb hemoglobin
HYPX hypoxanthine
IMP inosine monophosphate
INO inosine
LAC lactate
MetHb methemoglobin
P2G 2-phosphoglycerate
P3G 3-phosphoglycerate
PEP phosphenolpyruvate
PRPP 5-phosphoribosyl pyrophosphate
PYR pyruvate
R1P ribose-1-phosphate
R5P ribose-5-phosphate
RL5P ribulose-5-phosphate
SED7P sedoheptulose 7-phosphate
XYL5P xylose-5-phosphate

Abbreviations for reactions

AdylK adenylate kinase (EC 2.7.4.3)
ADA adenosine deaminase (EC 3.5.4.4)
ADPRT adenine phosphoribosyltransferase (EC 2.4.2.7)
AK adenosine kinase (EC 2.7.1.20)
ALD aldolase (EC 4.1.2.13)
AMPase adenosine monophosphate phosphohydrolase (EC 3.1.3.5)
AMPDA adenosine monophosphate deaminase (EC 3.5.4.6)
DPGase diphosphoglycerate phosphatase (EC 3.1.3.13)
DPGM diphosphoglycerate mutase (EC 5.4.2.4)
EN enolase (EC 4.2.1.11)
G6PDH glucose-6-phosphate dehydrogenase (EC 1.1. 1.49)
GAPDH glyceraldehyde-3-phosphate dehydrogenase (EC 1.2.1.12)
GL6PDH phosphogluconate dehydrogenase (EC 1.1.1.44)
GSSG-R glutathione-disulfide reductase (EC 1.8.1.7)
HGPRT hypoxanthine phosphoribosyltransferase (EC 2.4.2.8)
HK hexokinase (EC 2.7.1.1)
IMPase inosine monophosphate phosphohydrolase (EC 3.1.3.5)
LDH lactate dehydrogenase (EC 1.1.1.27)
MemPhos membrane phosphorylation
MetHbRed methemoglobin reductase
PFK phosphofructokinase (EC 2.7.1.11)
PGI glucose-6-phosphate isomerase (EC 5.3.1.9)
PGK phosphoglycerate kinase (EC 2.7.2.3)
PGLase phosphogluconolactonase (EC 3.1.1.31)
PGM phosphoglycerate mutase (EC 5.4.2.1)
PK pyruvate kinase (EC 2.7.1.40)
PNPase purine-nucleoside phosphorylase (EC 2.4.2.1)
PRM phosphoribomutase (EC 5.4.2.7)
PRPPsyn phosphoribosylpyrophosphate synthetase (EC 2.7.6.1)
RPI ribose-5-phosphate isomerase (EC 5.3.1.6)
TA transaldolase (EC 2.2.1.2)
TK transketolase (EC 2.2.1.1)
TPI triosephosphate isomerase (EC 5.3.1.1)
XPI ribulose phosphate epimerase (EC 5.1.3.1)

Appendix B. Supplementary data

Supplementary data associated with this article can be found, in the online version, at doi:10.1016/j.compbiolchem.2006.07.001.

References

Bonarius, H.P.J., Hatzimanikatis, V., Meesters, K.P.H., de Gooijer, C.D., Schmid, G., Tramper, J., 1996. Metabolic flux analysis of hybridoma cells in different culture media using mass balances. Biotechnol. Bioeng. 50, 299–318.

Bossi, D., Giardina, B., 1996. Red cell physiology. Mol. Aspects Med. 17, 117–128.

Çakır, T., Tacer, C.S., Ülgen, K.Ö., 2004. Metabolic pathway analysis of enzyme-deficient human red blood cells. BioSystems 78, 49–67.

Emmerling, M., Dauner, M., Ponti, A., Fiaux, J., Hochuli, M., Szyperski, T., Wuthrich, K., Bailey, J.E., Sauer, U., 2002. Metabolic flux responses to pyruvate kinase knockout in *Escherichia coli*. J. Bacteriol. 184, 64–154.

Förster, J., Famili, I., Fu, P., Palsson, B.O., Nielsen, J., 2003. Genome scale reconstruction of the Saccharomyces cerevisiae metabolic network. Genome Res. 13, 244–253.

Fujii, H., Miwa, S., 2000. Other erythrocyte enzyme deficiencies associated with non-hematological symptoms: phosphoglycerate kinase and phosphofructokinase deficiency. Best Pract. Res. Clin. Haematol. 13, 141–148.

Holzhütter, G.H., 2004. The principle of flux minimization and its application to estimate stationary fluxes in metabolic networks. Eur. J. Biochem. 271, 2905–2922.

Jacobasch, G., Rapoport, S.M., 1996. Hemolytic anemias due to erythrocyte enzyme deficiencies. Mol. Aspects Med. 17, 143–170.

Jacobasch, G., 2000. Biochemical and genetic basis of red cell enzyme deficiencies. Best Pract. Res. Clin. Haematol. 13, 1–20.

Jamshidi, N., Edwards, J.S., Fahland, T., Church, G.M., Palsson, B.O., 2001. Dynamic simulation of the human red blood cell metabolic network. Bioinformatics 17, 286–287.

Joshi, A., Palsson, B.O., 1989. Metabolic dynamics in the human red cell. Part I. A comprehensive kinetic model. J. Theor. Biol. 141, 515–528.

Kannoo, H., Fujii, H., Miwa, S., 1998. Expression and enzymatic characterization of human glucose phosphate isomerase (GPI) variants accounting for GPI deficiency. Blood Cell Mol. Dis. 24, 54–61.

Kauffman, K.J., Prakash, P., Edwards, J.S., 2003. Advances in flux balance analysis. Curr. Opin. Biotechnol. 14, 491–496.

Martinov, M.V., Plotnikov, A.G., Vitvitsky, V.M., Ataullakhanov, F.I., 2000. Deficiencies of glycolytic enzymes as a possible cause of hemolytic anemia. Biochim. Biophys. Acta 1474, 75–87.

Momsen, G., Vestergaard-Bogind, B., 1978. Human erythrocyte 2,3-diphosphoglycerate metabolism. Influence of 1,3-diphosphoglycerate and P_i. Arch. Biochem. Biophys. 190, 67–87.

Mulquiney, P.J., Kuchel, P.W., 1999. Model of 2,3-biphosphoglycerate metabolism in the human erythrocyte based on detailed enzyme kinetic equations: equations and parameter refinement. Biochem. J. 342, 581–596.

Ni, T.C., Savageau, M.A., 1996. Application of biochemical systems theory to metabolism in human red blood cells. J. Biol. Chem. 271, 7927–7941.

Olah, J., Orosz, F., Keserü, G.M., Kovari, Z., Kovacs, J., Hollan, S., Ovadi, J., 2002. Triosephosphate isomerase deficiency: a neurodegenerative misfolding disease. Biochem. Soc. Trans. 30, 30–38.

Orosz, F., Vertessy, B.G., Hollan, S., Horany, M., Ovadi, J., 1996. Triosephosphate isomerase deficiency: predictions and facts. J. Theor. Biol. 182, 437–447.

Price, N.D., Reed, J.L., Papin, J.A., Wiback, S.J., Palsson, B.O., 2003. Network based analysis of metabolic regulation in the human red blood cell. J. Theor. Biol. 225, 185–194.

Repiso, A., Boren, J., Ortega, F., Pujades, A., Centelles, J., Vives-Corrons, J.L., Climent, F., Cascante, M., Carreras, J., 2002. Triosephosphate isomerase deficiency: genetic, enzymatic, and metabolic characterization of a new case from Spain. Haematologica 87, e-cases.

Schilling, C.H., Palsson, B.O., 1998. The underlying structure of biochemical reaction networks. Proc. Natl. Acad. Sci. U.S.A. 95, 4193–4198.

Schneider, A.S., 2000. Triosephosphate isomerase deficiency: historical perspectives and molecular aspects. Best Pract. Res. Clin. Haematol. 13, 119–140.

Schuster, R., Jacobasch, G., Holtzhütter, H.G., 1989. Mathematical modelling of metabolic pathways affected by an enzyme deficiency. Energy and redox metabolism of glucose-6-phosphate-dehydrogenase-deficient erythrocytes. Eur. J. Biochem. 182, 605–612.

Schuster, R., Holtzhütter, G.H., 1995. Use of mathematical models for predicting the metabolic effect of large-scale enzyme activity alterations: application to enzyme deficiencies of red blood cells. Eur. J. Biochem. 229, 403–418.

Schuster, S., Fell, D.A., Pfeiffer, T., Dandekar, T., Bork, P., 1998. Elementary modes analysis illustrated with human red cell metabolism. In: Larsson, C., Pahlman, I.L., Gustafsson, L. (Eds.), BioThermoKinetics in the Post Genomic Era. Chalmers, Göteborg, pp. 332–339.

Segre, D., Vitkup, D., Church, G.M., 2002. Analysis of optimality in natural and perturbed metabolic networks. PNAS 99, 15112–15117.

Sheikh, K., Forster, J., Nielsen, L.K., 2005. Modeling hybridoma cell metabolism using a generic genome-scale model of Mus musculus. Biotechnol. Prog. 21, 112–121.

Shlomi, T., Berkman, O., Ruppin, E., 2005. Regulatory on/off minimization of metabolic flux changes after genetic perturbations. PNAS 102, 7695–7700.

Varma, A., Palsson, B.O., 1994. Metabolic flux balancing: basic concepts, scientific and practical use. Bio/Technology 12, 994–998.

Wiback, S.J., Palsson, B.O., 2002. Extreme pathway analysis of human red blood cell metabolism. Biophys. J. 83, 808–818.